

Thermal Decomposition of Trimethylamine Borane As a Precursor to Nanocrystalline CVD BC_xN_y Films

O. P. Korobeinichev^a, A. G. Shmakov^a, A. A. Chernov^a, M. L. Kosinova^b,
V. S. Sulyaeva^b, and F. A. Kuznetsov^b

^a Institute of Chemical Kinetics and Combustion, Siberian Branch, Russian Academy of Sciences,
Institutskaya ul. 3, Novosibirsk, 630090 Russia

^b Nikolaev Institute of Inorganic Chemistry, Siberian Branch, Russian Academy of Sciences,
pr. Akademika Lavrent'eva 3, Novosibirsk, 630090 Russia

e-mail: chernov@kinetics.nsc.ru

Received February 14, 2011

Abstract—We have studied the kinetics of BC_xN_y chemical vapor deposition through trimethylamine borane decomposition at atmospheric pressure. The rate constant of the heterogeneous interaction between trimethylamine borane and an adsorption center has been determined to be $k_s^0 = 2.7 \times 10^7 \exp(-10560/T)$ cm/s. The obtained kinetic parameters of the reaction fully determine the growth rate of nanocrystalline carbonitride films under kinetic control. The film thickness has been determined as a function of time, temperature, reactant concentration, and reactor dimensions.

DOI: 10.1134/S0020168511100128

INTRODUCTION

Although B–C–N ceramic materials have long been studied and have found industrial applications, the deposition and the physicochemical and mechanical properties of thin B–C–N films have attracted researchers' interest only in the past fifteen years.

Hexagonal (graphite-like) boron carbonitride ($h\text{-BC}_x\text{N}_y$) may be intermediate in properties between graphite (a good conductor) and $h\text{-BN}$ (dielectric) [1, 2]. BC_xN_y films are potentially attractive for basic technologies of next-generation memory devices and as protective coatings in semiconductor devices, e.g., in next-generation microprocessors [3].

Golubenko et al. [2] presented a theoretical analysis of the feasibility of boron carbonitride chemical vapor deposition (CVD) from trimethylamine borane (TMAB), $(\text{CH}_3)_3\text{N} : \text{BH}_3$. They used thermodynamic modeling to determine the vapor composition and identify the condensed phases in equilibrium with the vapor phase. According to their results, the set of condensed phases in equilibrium with the vapor phase depends to a significant degree on the initial composition of the vapor mixture and the deposition parameters. CVD from TMAB + nitrogen mixtures leads to the formation of BN + C mixtures over the entire range of conditions studied. Thus, in the case of TMAB + nitrogen mixtures, carbon (graphite) is deposited together with boron nitride.

Data on the chemistry of trimethylamine borane decomposition are not available in the literature.

The purpose of this work was to study the products and kinetics of TMAB decomposition in the CVD of nanocrystalline films.

EXPERIMENTAL

Trimethylamine borane was decomposed at atmospheric pressure in flowing nitrogen in a flow reactor (Fig. 1). We used boron hydride–trimethylamine manufactured by Merck (catalog no. 8.21915.0010). The furnace temperature was varied from 200 to 800°C, the heated volume in the reactor was 7.7 cm³, and the gas flow rate was 3 cm³/s. The TMAB content was 0.45%. The residence time of the substance in the flow reactor was 1–2 s.

These experimental conditions were chosen because TMAB actively decomposes not only in the vapor phase but also on the reactor wall. The products of the two TMAB decomposition paths are, most likely, identical. Based on general ideas of thermal unimolecular reactions [4], it is reasonable to assume that the transition pressure ($p_{1/2}$) for TMAB is below 10^{−5} atm. Therefore, TMAB decomposition in the vapor phase at a pressure of 1 atm is a unimolecular process [5].

The mean square mixing length in a flow reactor is $\bar{z}^2 = 2Dt$. At a flow rate of 5–6 cm³/s and a residence time in the reactor from 1 to 2 s, complete mixing takes 0.5–1 s. $R^2/(8D) = 0.09$ is much less than $2R/(\xi^*v)$ and ranges from 2 to 200 depending on temperature and ξ (R is the radius of the reactor, $D = 0.35 \pm$

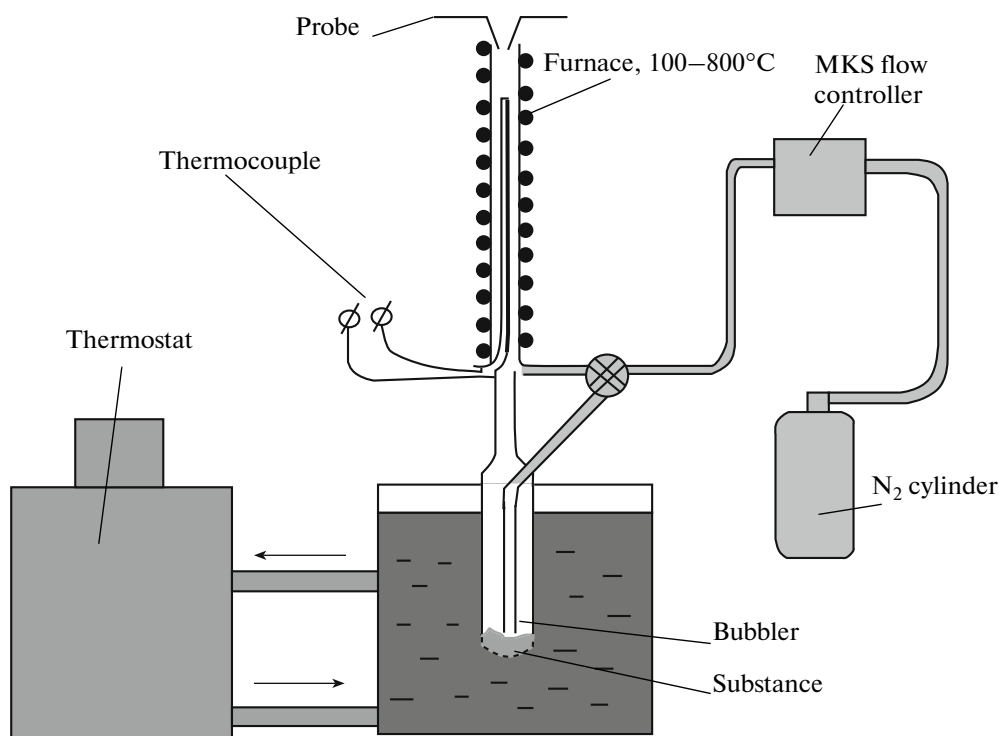
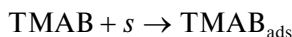


Fig. 1. Schematic of the flow reactor.

$0.05 \text{ cm}^2/\text{s}$ is the diffusion coefficient of TMAB in nitrogen, ξ is adsorption probability, and v is the average velocity of molecules). Therefore, the decomposition on the reactor wall is kinetically controlled. Accordingly, the decomposition rate on the wall will be determined by the rate of interaction with an adsorption center. The rate constant of the elementary reaction



is

$$k_s = (S/V)(v/4)\exp(-E_s/RT),$$

where E_s is the activation energy, S is the area of the wall, and V is the reactor volume.

Thus, TMAB decomposes as a result of concurrent processes. If the amount of adsorption centers far exceeds the initial amount of the substance, the rate equation for the decomposition process can be written in the form

$$d[\text{TMAB}]/dt = -k_s[\text{TMAB}] - k_m[\text{TMAB}].$$

Samples for analysis of decomposition products were taken 8 mm from the end of the reactor on its axis using a system that incorporated an MS7302 soft-ionization quadrupole mass spectrometer and molecular beam sampler [6]. The system has high sensitivity and enables one to measure low concentrations (down to 10 ppm) of not only stable but also labile substances (such as atoms and free radicals). The decomposition

products were also characterized by gas chromatography/mass spectrometry (GC/MS). To this end, a sample was taken at the reactor outlet and was then analyzed on an HP 5973 gas chromatograph/mass spectrometer equipped with a Valco six-port valve (0.25-ml sample loop). For chromatographic separation and analysis, we used an HP-5MS capillary column ($30 \text{ m} \times 0.25 \text{ mm}$). Samples were taken by freezing decomposition products from the reactor outlet in a nitrogen trap.

To obtain signal intensities for individual substances, one should know the contribution of each substance to the signal at a given ionization energy. We relied on the 70-eV contributions reported in the literature and calibrations at a reactor temperature of 373 K. To obtain signal intensities for individual substances, we subtracted contributions from the other substances. Some of the peaks were separated by another technique: by lowering the ionizing electron energy to the level where fragment peaks disappeared.

RESULTS AND DISCUSSION

Figures 2 and 3 present primary data on the intensity of mass peaks versus reactor temperature for a sample taken at the reactor outlet. Starting at 488 K, the intensity of the main peak (72 amu) in the mass spectrum of TMAB (parent peak at 73 amu) drops rather rapidly. At the same time, the peak at 59 amu rises rapidly with increasing reactor temperature. This

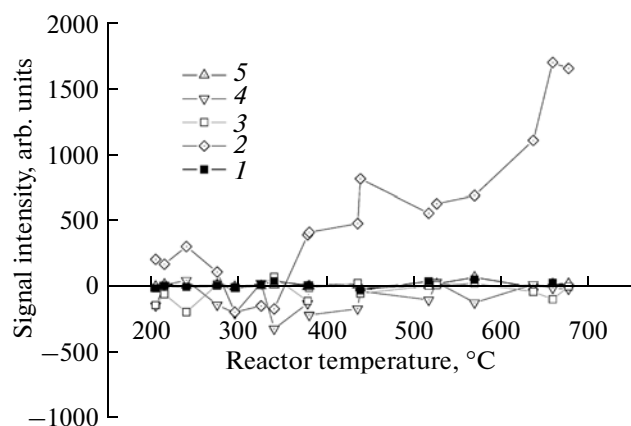


Fig. 2. Intensity of mass peaks at (1) 17, (2) 16, (3) 15, (4) 14, and (5) 13 amu as a function of reactor temperature.

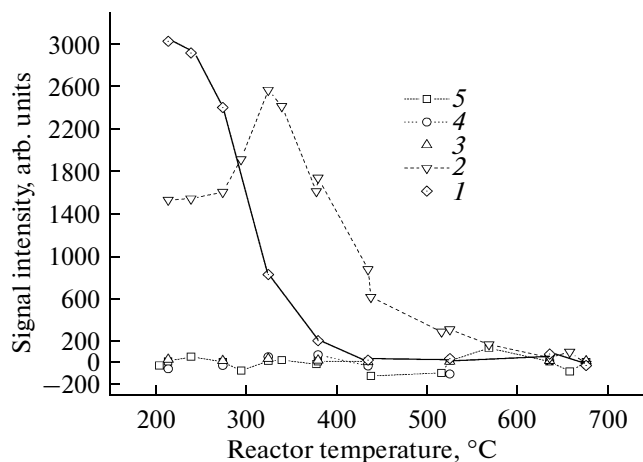


Fig. 3. Intensity of mass peaks at (1) 56, (2) 30, (3) 29, (4) 28 (13.5 eV), and (5) 25 amu as a function of reactor temperature.

peak is the main one in the spectrum of trimethylamine (TMA), $(\text{CH}_3)_3\text{N}$. Independent GC/MS analyses confirmed that TMA was the main TMAB decomposition product.

Figure 4 presents GC/MS analysis data for a sample taken at the reactor outlet.

Figure 5 shows the TMAB and decomposition product concentrations at the reactor outlet as functions of temperature. As seen, the TMAB concentration at the reactor outlet decreases rapidly with increasing temperature. In the range 488–650 K, TMAB decomposes almost completely, releasing TMA vapor. Its concentration peaks near 633 K, approaching the initial TMAB concentration. At this

temperature, we detect dimethylamine (DMA), $(\text{CH}_3)_2\text{NH}$, whose concentration peaks at 723 K. At 873 K, we observe a maximum in the signal intensity of another TMAB decomposition product: monomethylamine (MMA), $(\text{CH}_3)\text{NH}_2$. Starting at 633 K, the methane (CH_4) concentration at the reactor outlet increases steadily. There are also trace levels of BH_3 and ammonia. After each experiment, we find a carbon black deposit on the reactor wall. In mass spectra, carbon black or solid carbon cannot be detected. At the same time, the percentage of solid carbon can be determined using the carbon balance. This is quite justified and, since no carbon-containing products other than those mentioned above were detected, the per-

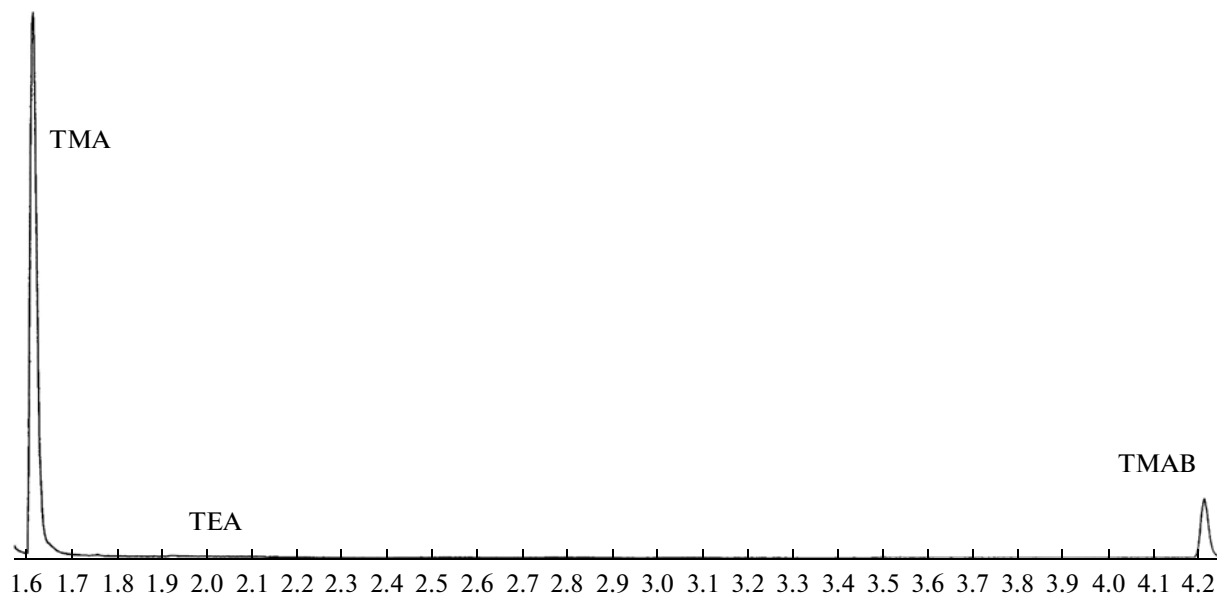


Fig. 4. GC/MS analysis data: $T_r = 523$ K, $p = 1$ atm.

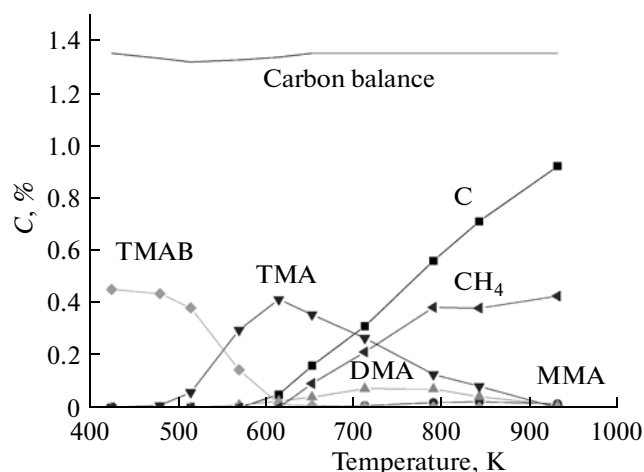


Fig. 5. TMAB and decomposition product concentrations at the reactor outlet as functions of temperature.

centage of solid carbon can be determined using the carbon balance.

To determine the order of the reaction, we measured the degree of TMAB decomposition as a function of initial concentration at a reactor temperature of 573 ± 7 K. The degree of decomposition in this temperature range was found to be $\sim 50 \pm 2\%$. The initial trimethylamine borane concentration was varied by changing the bubbler temperature. The carrier gas flow rate was $3.27 \text{ cm}^3/\text{s}$ (at 293 K).

Figure 6 plots the degree of TMAB decomposition under these conditions versus initial TMAB concentration. Experimental data demonstrate that TMAB decomposition is a first-order reaction. Using these data, we can find parameters of an effective TMAB thermolysis reaction. Under the assumption that the

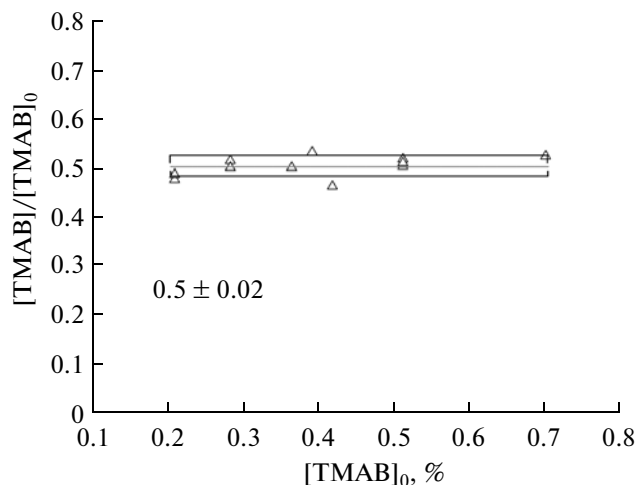
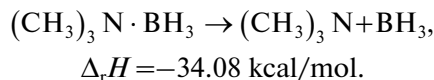


Fig. 6. Degree of TMAB decomposition as a function of initial TMAB concentration.

reaction is first-order, the variation in TMAB concentration is given by

$$A/A_0 = \exp(-k\tau),$$

where A is the mole fraction of TMAB at the reactor outlet, A_0 is the initial TMAB concentration, and τ is the residence time in the reactor. If the initial step of TMAB decomposition is BH_3 removal and trimethylamine formation, we can evaluate the energetics of the reaction using earlier data [7–12]:



According to Issoire and Long [8], the enthalpy of TMAB formation is -20 kcal/mol . Tel'noi and Rabinovich [9] also calculated the enthalpy of TMAB formation: -14.28 kcal/mol . We used these data. As a result, TMAB decomposition was shown to be an endothermic reaction. Accordingly, the activation energy for the unimolecular decomposition reaction in the vapor phase should exceed 34 kcal/mol and should be $\sim 40 \text{ kcal/mol}$.

Figure 7 compares the TMAB concentration profiles calculated for different activation energies and preexponential factors. As seen, the dominant step of the process at temperatures below 650 K is TMAB decomposition on the reactor wall. The unimolecular decomposition reaction in the vapor phase can compete with this process only at higher temperatures.

Figure 8 shows Arrhenius plots of the TMAB decomposition rate constant. At temperatures above 675 K , the rate constant of the unimolecular decomposition in the vapor phase increases markedly. Clearly, 675 K is the optimal temperature for chemical vapor deposition.

From the above results, we estimated the enthalpy of TMAB adsorption on quartz glass: $\Delta H = 21.12 -$

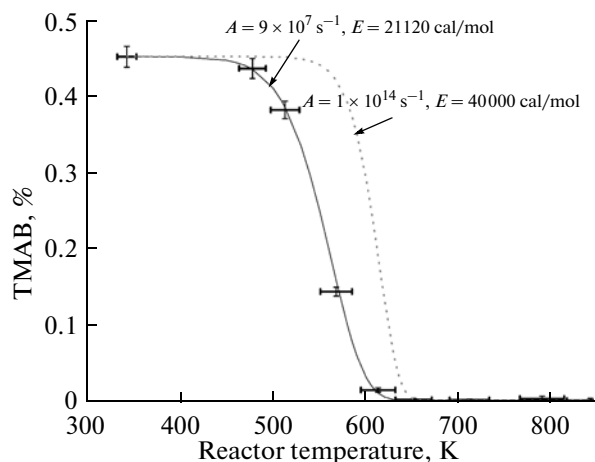


Fig. 7. Degree of TMAB decomposition as a function of reactor temperature. The points represent experimental data and the curves represent calculation results.

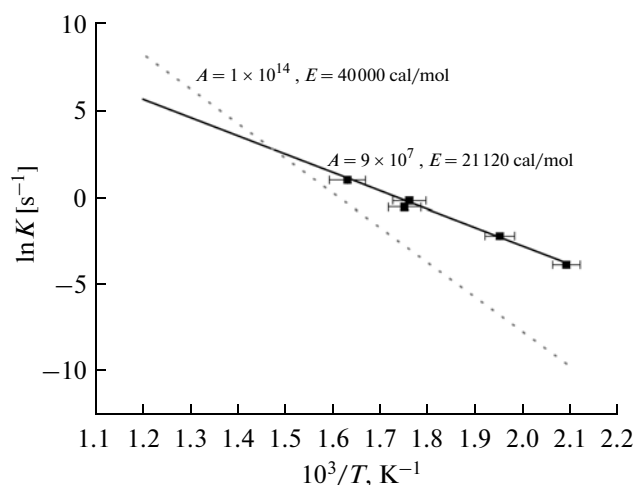


Fig. 8. Arrhenius plots of the decomposition rate constant. The points represent experimental data.

40 = −18.88 kcal/mol. We can also determine the rate constant of the elementary reaction between TMAB and an adsorption center. To this end, the effective decomposition rate constant, k_s , should be divided by the ratio of the reactor area to its volume (3.35). In this way we find that the rate constant of the heterogeneous reaction is

$$k_s^0 = 2.7 \times 10^7 \exp(-21120/RT) \text{ cm/s.}$$

When heterogeneous TMAB decomposition prevails, the thickness of the film as a function of time and temperature is proportional to the rate of interaction with adsorption centers:

$$L(t) = V^*[\text{TMAB}] [V_r/S_r] (1 - \exp(S_r k_s^0 t/V_r)).$$

Here, $V^* = 10^{-21} \text{ cm}^3$ is the average “packing” size; $[\text{TMAB}]$ is the TMAB concentration (molecule/ cm^3); S_r and V_r are the reactor area and volume, respectively; and t is the deposition time.

At $p = 3.9 \text{ Pa}$, $T = 670 \text{ K}$, a TMAB content of 5% in the mixture with nitrogen, and an average molecular size in the film of 10^{-21} cm^3 , the film growth rate is 10 nm/min, in good agreement with earlier data [13].

Figure 9 is a scanning electron microscopy image of a film grown on a quartz glass substrate. The substrate was mounted at the reactor outlet, and the reactor and substrate temperatures were maintained at 723 K. Analysis showed that the film was inhomogeneous and consisted of thin “fibers” and dense zones, lending support to our assumption that there were two TMAB decomposition paths. Elemental analyses of the film showed that the fibers contained no nitrogen. It seems, therefore, likely that the dense zones result from decomposition in reactions with adsorption centers on the substrate surface and that the fibers result from the formation of BH_3 and carbon black in the vapor phase, which then adsorb on the substrate. According to

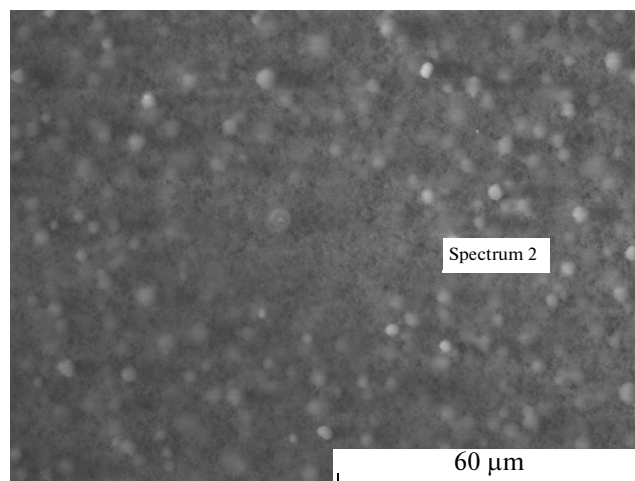


Fig. 9. Electron micrograph of a condensed phase deposited onto a quartz substrate.

energy dispersive X-ray spectroscopy, the B : C : N atomic ratio in the fibers is 3 : 1 : 10. The B : C : N atomic ratio in the dense zones is 7.8 : 2.6 : 1.

The set of condensed phases in films depends to a significant degree on the initial vapor mixture composition and temperature [2]. According to thermodynamic modeling results, the phase forming at low temperatures (<500 K) is boron nitride. At temperatures above 1055 K, a three-phase mixture, $\text{BN} + \text{C} + \text{B}_4\text{C}$, forms. Its elemental composition indicates that the fibers consist mainly of $\text{C} + \text{B}_4\text{C}$.

It can be seen from Fig. 5 that the fraction of carbon in the solid phase varies considerably with temperature. At 723 K, it reaches 20% of the total amount of carbon in TMAB. A similar situation holds in the case of nitrogen: more than 80% of the nitrogen atoms leave the reactor in the form of TMA vapor, without depositing on the substrate. The film forming under such conditions consists of three phases in dense zones, with a BN : C : B_4C ratio of 12 : 10 : 21.

CONCLUSIONS

We have studied the products and kinetics of TMAB decomposition in flowing nitrogen in a flow reactor.

The kinetic parameters of the rate constant of TMAB adsorption on quartz have been determined as functions of temperature. These parameters fully determine the growth rate of nanocrystalline carbonitride films under kinetic control.

TMAB decomposition is a first-order reaction.

The first step of the process is TMAB adsorption on the reactor wall. The next step is BH_3 removal and the formation of trimethylamine at temperatures below 650 K or a three-phase film at higher temperatures.

REFERENCES

1. Kuznetsov, F.A., et al., Materials and Basic Technologies of Next-Generation Electronic Devices: Dielectric Layers, *Izv. Vyssh. Uchebn. Zaved., Mater. Elektron. Tekh.*, 2007, vol. 4, pp. 54–62.
2. Golubenko, A.N., Kosinova, M.L., Titov, A.A., and Kuznetsov, F.A., Thermodynamic Modeling of BC_xN_y Chemical Vapor Deposition in the B–C–N–H System, *Inorg. Mater.*, 2003, vol. 39, no. 4, pp. 362–365.
3. Baake, O., Hoffmann, P.S., Klein, A., et al., Chemical Character of BC_xN_y Layers Grown by CVD with Trimethylamine Borane, www.interscience.wiley.com/journal/xrs, Wiley, 2008.
4. Robinson, P.J. and Holbrook, K.A., *Unimolecular Reactions*, London: Wiley, 1972. Translated under the title *Monomolekulyarnye reaktsii*, Moscow: Mir, 1975, pp. 125–127.
5. Kosinova, E.A., Sulyaeva, V.S., and Sysoev, S.V., Temperature-Dependent Triethylamine Borane Vapor Pressure, *XLI Mezhdunarodnaya nauchnaya studentskaya konferentsiya "Student i nauchno-tehnicheskii progress" (Khimiya)* (XLI Int. Scientific Student Conf.: Student and Progress in Science and Technology (Chemistry), Novosibirsk, 2003, pp. 145–146.
6. Chernov, A.A., Korobeinichev, O.P., Shvartsberg, V.M., and Mokrushin, V.V., Destruction of Trimethyl Phosphate in $H_2/O_2/Ar$ Flame, *26th Int. Symp. on Combustion*, Pittsburgh, PA: Combustion Institute, 1996, pp. 1035–1042.
7. Chase, M.W., NIST–JANAF Thermochemical Tables, Fourth Edition, *J. Phys. Chem. Ref. Data*, 1998, monograph 9, p. 1–1951.
8. Issoire, J. and Long, C., Etude de la thermodynamique chimique de la reaction de formation des methyamines, *Bull. Soc. Chim. Fr.*, 1960, pp. 2004–2012.
9. Tel'noi, V.I. and Rabinovich, I.B., Thermal Chemistry of Main Group Element Organic Compounds, *Usp. Khim.*, 1980, vol. 49, no. 7, pp. 1137–1173.
10. Sana, M., Leroy, G., and Wilante, C., Enthalpies of Formation and Bond Energies in Lithium, Beryllium, and Boron Derivatives: 2. Dative, Single, and Triple Bonds, *Organometallics*, 1992, vol. 11, no. 2, pp. 781–787.
11. Leroy, G., Sana, M., and Wilante, C., Evaluation of the Bond Energy Terms for the Various Types of Boron–Nitrogen Bonds, *Theor. Chem. Acta*, 1993, no. 85, pp. 155–166.
12. Grant, J., et al., Revised Heat of Formation for Gaseous Boron: Basis Set Limit Ab Initio Binding Energies of BF_3 and BF , *Phys. Chem. A*, 2009, vol. 113, pp. 6121–6132.
13. Kosinova, M.L., Rummyantsev, Yu.M., Golubenko, A.N., et al., Chemical Composition of Boron Carbonitride Films Grown by Plasma-Enhanced Chemical Vapor Deposition from Trimethylamineborane, *Inorg. Mater.*, 2003, vol. 39, no. 4, pp. 366–373.